Turkish Journal of Agriculture - Food Science and Technology, 13(s2): 3529-3524, 2025
DOI: https://doi.org/10.24925/turjaf.v13is2.3529-3524.8093

Turkish Journal of Agriculture - Food Science and Technology

Available online, ISSN: 2148-127X | www.agrifoodscience.com | Turkish Science and Technology Publishing (TURSTEP)

Double-Layer Coated TiO_2 Structures Derived from an Agro-Industrial Biowaste: A Comprehensive Characterization for Water Treatment

Nazli Türkten[1,a,*], Yunus Karatas[1,b], Yelda Yalcin Gurkan[2,c], Zekiye Cinar[3,d]

[1]*Kirsehir Ahi Evran University, Faculty of Arts and Sciences, Department of Chemistry, 40100, Kirsehir, Türkiye*
[2]*Tekirdag Namik Kemal University, Faculty of Arts and Sciences, Department of Chemistry, 59030, Tekirdag, Türkiye*
[3]*Yildiz Technical University, Faculty of Arts and Sciences, Department of Chemistry, 34220, Istanbul, Türkiye*
[*]*Corresponding author*

ARTICLE INFO

Research Article

Received : 12.07.2025
Accepted : 11.08.2025

Keywords:
Agricultural Waste
Bio template
Photocatalysis
Risk Husk
Sol-Gel

ABSTRACT

Recently, the use of agro-industrial biowaste, particularly rice husk (RH), has emerged as a promising option for producing value-added products. This low-cost solid waste is considered a potential multi-dopant source and a green approach for preparing photocatalysts used in water treatment. Double-layer coated TiO_2 (RH2xTiO_2) structures derived from RH were synthesized through the sol-gel process. RH acted as both an agro-industrial biowaste template and a multi-dopant ion source during the double-layer coating process of TiO_2. The sacrifice of this template in the calcination process resulted in the formation of a self-doped catalyst containing silicon, carbon, nitrogen, and sulfur. The characterization features of the photocatalyst were carried out by using XRD, SEM, XPS, BET, and UV-DRS spectroscopic techniques. The results of XRD analysis revealed that a mixture of anatase and rutile phases of TiO_2. The calculated crystallite particle size of RH2xTiO_2 structures was 18.4 nm. The SEM image of the RH2xTiO_2 structures exhibited a variety of polyhedral morphologies with cracks. The bang gap energy (E_{bg}) of the RH2xTiO_2 structures was 2.92 eV. BET analysis indicated that the RH2xTiO_2 specimen exhibited a Type IV isotherm, and the surface area was 77 m^2/g. The photocatalytic activity of RH2xTiO_2 structures was evaluated for the degradation of 4-nitrophenol (4-NP) as a model pollutant under UV irradiation.

[a] *nazli.turkten@yahoo.com* *https://orcid.org/0000-0001-9343-3697*
[b] *ykaratas@ahievran.edu.tr* *https://orcid.org/0000-0002-3826-463X*
[c] *yyalcin@nku.edu.tr* *https://orcid.org/ 0000-0002-8621-2025*
[d] *cinarz@yildiz.edu.tr* *https://orcid.org/ 0009-0008-0377-6126*

Introduction

Nowadays, the excessive production of agricultural waste is a major concern due to its potential for long-term environmental issues. Abundant agricultural residues can contaminate both water and soil quality, leading to adverse impacts (Mujtaba et al., 2023). Rice husk (RH) is a major agricultural waste processed particularly by the rice milling industry, which annually produces 600 million tons of rice as a staple food (Nzereogu et al., 2023). The difficulty of decomposing RH leads to an accumulation problem of RH on land. The open burning activity of RH results in the emission of carcinogenic gases. Hence, it is essential to utilize this agricultural waste as a cost-effective resource to produce value-added materials that can be used in industrial applications within the circular economy (Steven et al., 2021). The conversion of RH to silica materials is a viable option since it contains silica in amounts ranging from 5% to 30%, which varies based on the type of rice and its geographical origin. The extracted silica from RH concerns interest in potential technological applications such as reinforcing agents, fillers, filters, ceramics, refractory materials, and glass (Akhter et al., 2023; Kordi et al., 2024; Nzereogu et al., 2023; Singh Karam et al., 2022). Furthermore, RH is used as fuel for electricity and steam generation, as well as for producing biochar, adsorbents, and catalysts in water treatment processes (Kordi et al., 2024; Li et al., 2023; Okoro et al., 2022; Turkten et al., 2023).

Nitroaromatic compounds are commonly used in the production of explosives, dyes, pesticides, and herbicides. Among nitrophenols, 4-nitrophenol (4-NP) is a primary blacklisted contaminant due to its toxicity to microorganisms, mutagenic potential, and difficulty in degradation. The prolonged exposure to low levels of 4-NP can result in blood disorders and other health issues in humans. Additionally, certain concentrations of 4-NP found in groundwater and soil may pose risks to human health. Hence, it is crucial to eliminate this aromatic compound from wastewater before it contaminates groundwater (Ghosh et al., 2010; Zhang et al., 2024; Zhang et al., 2018).

Several attempts have been performed on the removal of 4-NP from modeled water, such as physicochemical, chemical, and biological techniques (El Messaoudi et al., 2024; Qatan et al., 2024; San et al., 2002). Photocatalysis represents a promising energy-efficient method to mineralize organic contaminants in a mild environment. This approach involves two key components: a photocatalyst and a light source. TiO_2 is the most well-known and reported conventional metal oxide semiconductors (Maridevaru et al., 2022; Motamedi et al., 2022).

To date, TiO_2-based photocatalysts have been used to mineralize 4-NP. San et al. investigated the predicted reaction paths through transition state theory (San et al., 2002). In the experimental part of the study, the effects of the parameters such as TiO_2 amount, 4-NP concentration, addition of H_2O_2 and Cu^{2+} ions on the degradation rate were determined. In another computational and experimental photocatalytic study, the photocatalytic activity of a series of iron-doped TiO_2 particles was investigated for the degradation of 4-NP, and DFT results indicated a substitutional Fe^{3+} doping of TiO_2 crystal (Yalçın et al., 2010a). Yalcin et al. reported that N, C, and S-doped TiO_2 particles enhanced the visible light activity, and these non-metal photocatalysts resulted in higher photocatalytic 4-NP degradation compared to undoped TiO_2 (Yalçın et al., 2010b). Besides, Se (IV) doped TiO_2, Se/N Co doped TiO_2 particles were prepared via wet impregnation method, and an enhanced photocatalytic degradation of 4-NP was also reported (Gurkan et al., 2017; Gurkan et al., 2013).

Recently, silica shell-derived TiO_2 and rice husk-templated TiO_2 particles have been studied (de Cordoba et al., 2019; Turkten et al., 2023; Wang et al., 2019; Zhang et al., 2017). Generally, the presence of silicon, carbon, nitrogen, and sulfur in RH is expected to facilitate self-multi-doping of TiO_2 catalysts during calcination, which is anticipated to improve light absorption. Zhang et al. synthesized double-shelled TiO_2 hollow spheres by using the hydrothermal method (Zhang et al., 2017). Ghamarpoor et al. extracted silica from RH and prepared nitrogen and carbon-doped TiO_2@SiO_2 core-shell nanostructures, and then prepared acrylic smart films to test the photocatalytic and self-cleaning performance (Ghamarpoor et al., 2025). In another photocatalytic study, mesoporous SiO_2@TiO_2 was prepared, resulting in a high degradation of Rhodamine B (Wang et al., 2019). Additionally, previous studies have reported that RH was used as a silica source to prepare TiO_2 photocatalysts (Banu Yener & Helvacı, 2015; de Cordoba et al., 2019; Hui et al., 2015; Liou et al., 2024; Liou & Wang, 2025; Zhaohui et al., 2018). In our previous study, we prepared a TiO_2 hierarchical microstructure by using RH as a biotemplate through a sol-gel method (Turkten et al., 2023). It was found that RH scarification led to multi-self-doped TiO_2 containing silicon, carbon, nitrogen, and sulfur. Our results indicated that the prepared TiO_2 structures derived from RH exhibited enhanced photocatalytic activity compared to TiO_2 nanoparticles.

The motivation for this study originated from our previous research, preparing and characterizing TiO_2 structures derived from RH (Turkten et al., 2023). This study was built upon to continue using RH as a biotemplate and prepared double-layer coated TiO_2 ($RH2xTiO_2$) structures via the sol-gel method. In this context, the structural, morphological, optical, and surface features of the double-layer coated TiO_2 photocatalyst derived from RH were discussed in detail. The photocatalytic activity of $RH2xTiO_2$ structures was evaluated using the model organic pollutant, 4-NP, under UV light irradiation.

Materials and Methods

Materials

RH, as a biotemplate material for synthesizing $RH2xTiO_2$ structures, was obtained from Kastamonu, Türkiye. Titanium (IV) isopropoxide (Aldrich), ethanol (Merck), 4-NP (Merck), and hydrochloric acid (Merck) were reagent grade and used without further purification.

Methods

Double-layer coated TiO_2 structures derived from RH were synthesized via a sol-gel modified method. The first layer of TiO_2 structures was synthesized as reported in our previous study (Turkten et al., 2023). Briefly, 0.1 mol titanium (IV) isopropoxide in 100 mL of ethanol was placed in a dropping funnel (Solution A). Deionized water (10 mL), acetic acid (10 mL), and ethanol (80 mL) were placed in a flat-bottomed flask (Solution B). Then, Solution A was added to Solution B under stirring, ensuring the pH remained at pH=2 with hydrochloric acid solution. RH (2 g) was dissolved in 10 mL of deionized water and placed in a beaker. This solution was then added to the prepared TiO_2 sol and stirred for 20 h. Afterwards, the solution was aged for 24 h, dried at 105°C. and washed. The same procedure was repeated for the preparation of the second layer. Finally, the obtained particles were calcined at 500°C for 5h to prepare $RH2xTiO_2$ structures.

Characterization

Detailed information on the characterization methods was thoroughly reported in our previous study (Turkten et al., 2023). The crystallite size of $RH2xTiO_2$ structures was calculated using the Scherrer equation (Eq. (1)) (Scherrer, 1918).

$$D = K\lambda / (\beta \cos\theta) \quad (1)$$

were,

K : 0.9,

λ : X-ray wavelength (1.5418 Å),

θ : Bragg angle, and

B : full width at half maximum intensity (FWHM, radians)

The band-gap energy of the $RH2xTiO_2$ structures was calculated using the Kubelka-Munk equation (Eq. (2)) (Kubelka & Munk, 1931).

$$(R) = (1-R)^2/2R \quad (2)$$

were,

R : Reflectance read from the spectrum.

Results and Discussion

The characteristics of RH and RH-derived TiO_2 specimens were identified and presented in our previous study (Turkten et al., 2023). The structural, morphological, optical, and surface properties of $RH2xTiO_2$ specimen were characterized.

The diffractogram of RH2xTiO$_2$ structures exhibited both anatase (JCPDS No. 73–1764) and rutile phases (JCPDS No. 99–0090) (Figure 1 (a)). The diffraction peaks of RH2xTiO$_2$ specimen at 2θ=25.39°, 38.01°, 38.82°, 48.32°, 54.47°, 55.21°, 62.76°, 69.16° corresponded to the (1 0 1), (0 0 4), (1 1 2), (2 0 0), (1 0 5), (2 1 1), (0 0 2), and (1 1 6) reflection planes of anatase, respectively, while 2θ=27.60°, 36.22°, 41.42°, 44.30°, 56.74° related to the (1 1 0), (1 0 1), (1 1 1), (2 1 0), and (2 0 0) reflection planes of rutile, respectively. The crystallite particle size of RH2xTiO$_2$ structures was 18.4 nm, which was a higher value (16.6 nm) compared to RH-derived TiO$_2$ specimens (Turkten et al., 2023). This result could indicate that the double coating caused an increase in crystallite particle size.

The SEM image of the RH2xTiO$_2$ specimen revealed different sizes of polyhedral morphology with cracks (Figure 1 (b)). The observed cracks found on the surface could be attributed to the removal of RH as a sacrificial template. The hierarchical structural morphology of RH was mostly protected in the SEM image of the RH-derived TiO$_2$ specimen (Figure 1 (c)). The double-layer coating could result in more aggregated particles on the surface compared to RH-derived TiO$_2$. The EDAX elemental weight distribution of the RH2xTiO$_2$ specimen consisted of Ti, O, Si, C, N, and S elements, containing amounts of 59.6%, 30.7%, 0.3%, 2.4%, 6.9%, and 0.1%, respectively.

The XPS spectrum of Ti 2p exhibited two photo-splitting peaks at 458.38 eV and 464.28 eV corresponding to the Ti 2p$_{1/2}$ and Ti 2p$_{3/2}$, respectively, confirming Ti^{4+} state bonding with oxygen. (Figure 2 (a)). The O 1s binding energy peak at 529.48 eV could be related to the metallic oxides (Figure 2 (b)). For the C 1s core level (Figure 2 (c)), a characteristic peak at 284.48 eV could belong to the C sp^2 graphitic carbon (Turkten et al., 2023).

According to IUPAC classification, the nitrogen adsorption-desorption isotherm of RH2xTiO$_2$ specimen (Figure 3 (a)) exhibited a Type IV isotherm (Sing, 1985). BJH surface area of RH2xTiO$_2$ structures was 77 m^2/g. The pore size and the total volume of RH2xTiO$_2$ specimen were 35 Å and 0.139 cm^3/g, respectively. The pore size distribution curve of RH2xTiO$_2$ structures was in the 20 Å - 40 Å region, indicating a mesoporous distribution (Figure 3 (b)). Yener et al. synthesized TiO$_2$/SiO$_2$ composites using extracted SiO$_2$ from RH as a silica support during the acid hydrolysis of TiCl$_4$. They reported that the surface areas were 180 m^2/g and 285 m^2/g, indicating both a micro- and mesoporous pore structure (Banu Yener & Helvacı, 2015). Yang et al. prepared RH-derived hierarchical porous TiO$_2$/SiO$_2$, exhibiting a surface area of 160 m^2/g (Yang et al., 2014). In our previous study, the surface area of RH-derived TiO$_2$ specimen was 55 m^2/g, which was smaller than RH2xTiO$_2$ structures (Turkten et al., 2023). The synthesis procedure and the double coating layer could cause differences in surface area values.

The UV-DRS spectrum of RH2xTiO$_2$ exhibited an absorption edge at around 330 nm and continued to approximately 450 nm (Figure 4 (a)). The E_{bg} value of the RH2xTiO$_2$ structures was 2.92 eV (λ = 425 nm), which was a lower value than the E_{bg} of TiO$_2$ nanoparticles (3.04 eV) reported in our previous study (Turkten et al., 2023). This finding indicated that double-coated process using RH as a multi-dopant ion resulted in a decline in the E_{bg} and a red shift was observed.

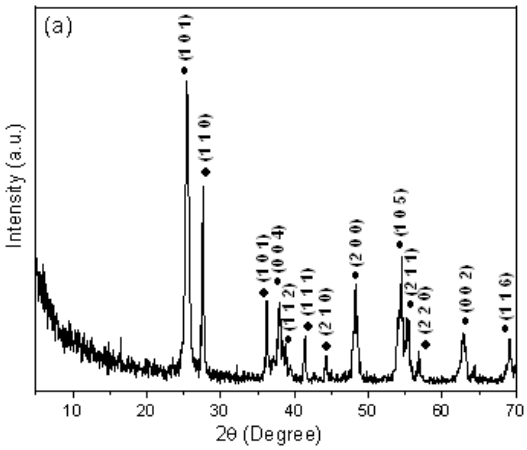

Figure 1. (a) XRD diffractogram (●anatase, ♦rutile), SEM images of the (b) RH2xTiO$_2$, and (c) RH-derived TiO$_2$ specimens.

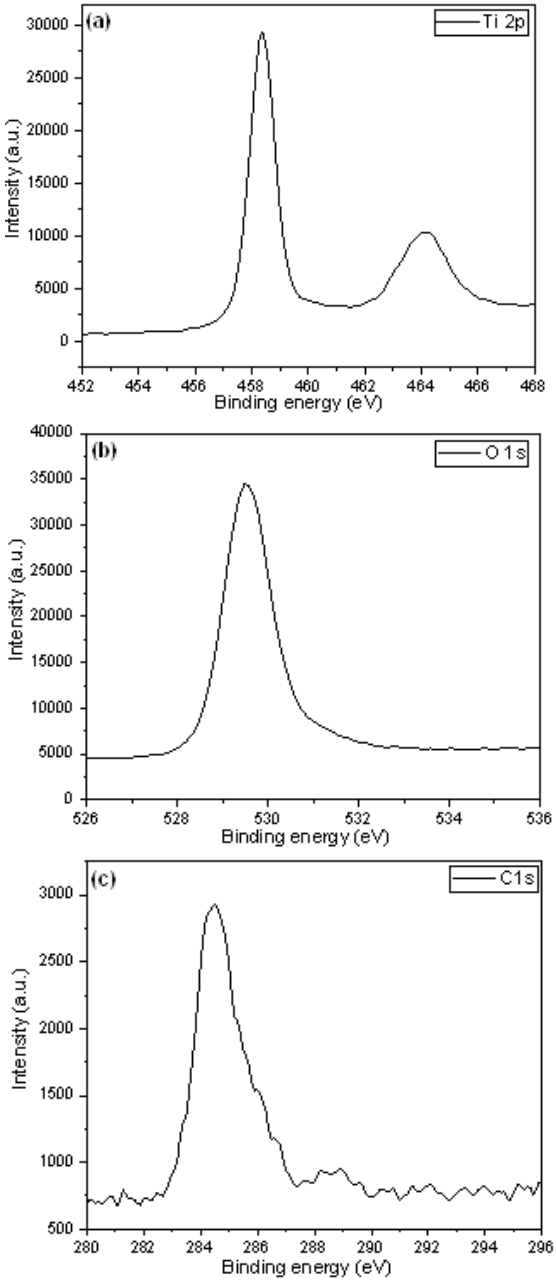

Figure 2. XPS spectra of (a) Ti 2p, (b) O 1s, and (c) C 1s of RH2xTiO$_2$ specimen.

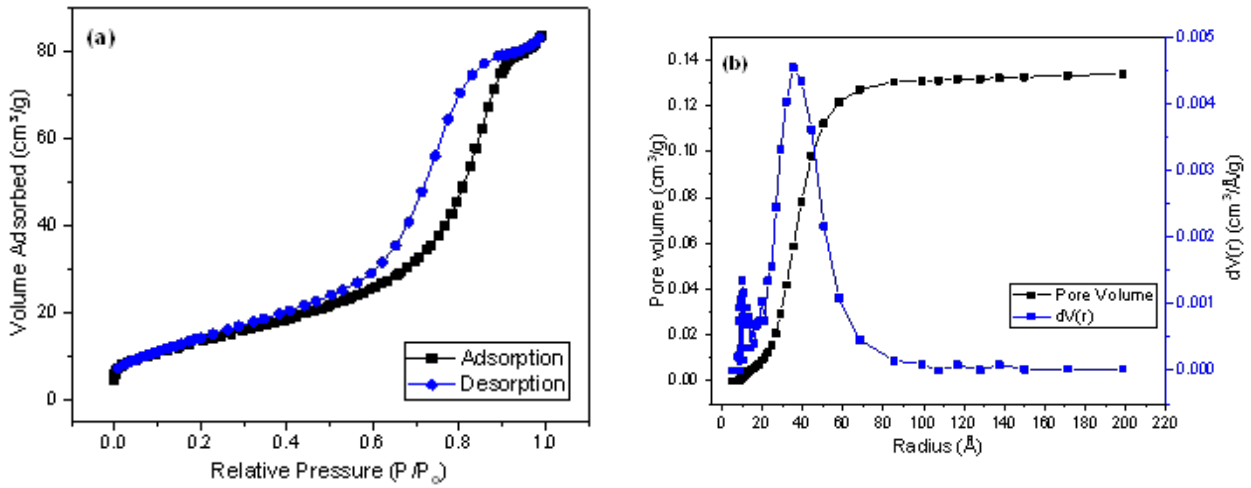

Figure 3. RH2xTiO$_2$ specimen of (a) N2 adsorption-desorption isotherm and (b) pore size distribution plot.

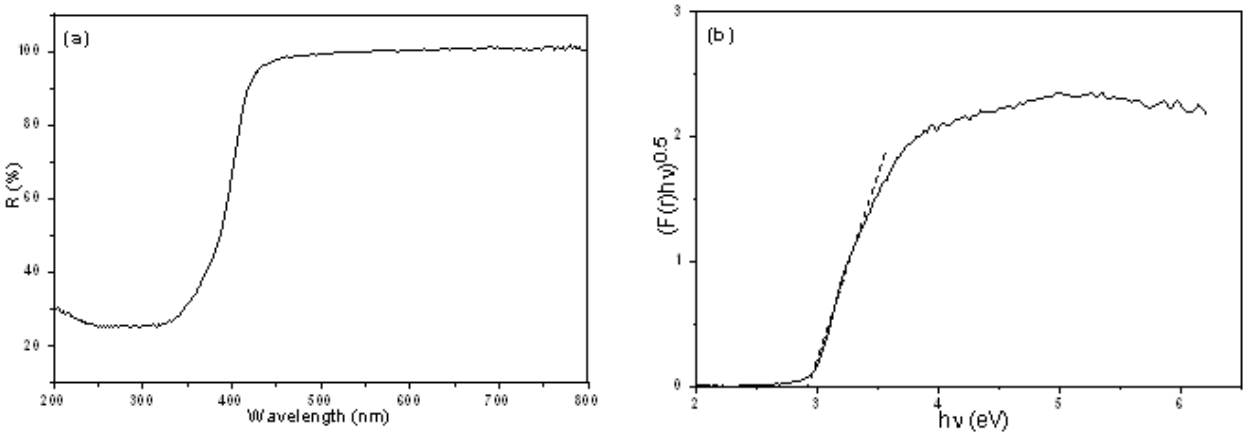

Figure 4. (a) UV-DRS spectrum of RH2xTiO$_2$ specimen and (b) (F(R).hν)0.5 v/s hν spectrum of RH2xTiO$_2$ specimen.

The photocatalytic activity test of the RH2xTiO$_2$ specimen (0.5 g/100mL) was performed in 600 mL of 4-NP (1x10^{-4} mol/L) solution in a Pyrex double-jacket photoreactor under UV-A irradiation. Blacklight fluorescent lamps (5 × 8 W) with a maximum at 365 nm were used as the light source. The reaction temperature (23±2 ºC) was maintained at a constant level using a water bath connected to a pump. The photocatalytic activity of the RH2xTiO$_2$ specimen on the degradation of 4-NP was carried out under UV light irradiation, and the removal efficiency of 4-NP was 27% after 120 min. It is well established that a larger surface area and a smaller crystallite size result in improved photocatalytic activity (Kim et al., 2007). The low photocatalytic activity is attributed not only to crystallite size and surface area but also to the aggregation of particles on the catalyst surface.

Conclusion

RH2xTiO$_2$ structures derived from RH as an agro-industrial biowaste, were prepared via a sol-gel method. RH served as both a template and a multi-dopant ion source for the double-layer coating process of TiO$_2$. The crystallite particle size of RH2xTiO$_2$ specimen was 18.4 nm. XRD analysis revealed the existence of both anatase and rutile phases of TiO$_2$. The isotherm of RH2xTiO$_2$ structures was Type IV and the pore size of the structures was 35 Å. The morphology of the RH2xTiO$_2$ specimen consisted of various sizes of polyhedral-shaped structures, which contained surface cracks due to RH removal. The E_{bg} value of the RH2xTiO$_2$ structures was 2.92 eV and red-shifted to comparable to that of TiO$_2$. The removal efficiency of 4-NP was found 27% in the presence of RH2xTiO$_2$ specimen. The results of this study have opened new prospects for the use of an abundant agro-industrial biowaste to a value-added, promising photocatalyst in water treatment.

Declarations

Ethical Approval Certificate

Not applicable.

Author Contribution Statement

N.T.: Conceptualization, investigation, formal analysis, writing the original draft, review and editing

Y.K.: Methodology, writing the original draft, review and editing

Y.Y.G.: Methodology, writing the original draft, review and editing

Z.C.: Supervision, conceptualization, investigation, writing the original draft

Fund Statement

There is no financial support and commercial support.

Conflict of Interest

The authors declare that they have no conflict of interest.

Acknowledgments

The present article is dedicated to the memory of Prof. Dr. Zekiye Cinar, who passed away on July 22, 2021.

References

Akhter, F., Soomro, S. A., Jamali, A. R., Chandio, Z. A., Siddique, M., & Ahmed, M. (2023). Rice husk ash as green and sustainable biomass waste for construction and renewable energy applications: a review. *Biomass Conversion and Biorefinery*, *13*(6), 4639–4649. https://doi.org/10.1007/s13399-021-01527-5

Banu Yener, H., & Helvacı, Ş. Ş. (2015). Effect of synthesis temperature on the structural properties and photocatalytic activity of TiO_2/SiO_2 composites synthesized using rice husk ash as a SiO_2 source. *Separation and Purification Technology*, *140*, 84–93. https://doi.org/https://doi.org/10.1016/j.seppur.2014.11.013

de Cordoba, M. C. F., Matos, J., Montaña, R., Poon, P. S., Lanfredi, S., Praxedes, F. R., Hernández-Garrido, J. C., Calvino, J. J., Rodríguez-Aguado, E., Rodríguez-Castellón, E., & Ania, C. O. (2019). Sunlight photoactivity of rice husks-derived biogenic silica. *Catalysis Today*, *328*, 125–135. https://doi.org/https://doi.org/10.1016/j.cattod.2018.12.008

El Messaoudi, N., Miyah, Y., Benjelloun, M., Georgin, J., Franco, D. S. P., Şenol, Z. M., Ciğeroğlu, Z., El Hajam, M., Knani, S., & Nguyen-Tri, P. (2024). A comprehensive review on designing nanocomposite adsorbents for efficient removal of 4-nitrophenol from water. *Nano-Structures & Nano-Objects*, *40*, 101326. https://doi.org/https://doi.org/10.1016/j.nanoso.2024.101326

Ghamarpoor, R., Jamshidi, M., Fallah, A., & Neshastehgar, M. (2025). Designing a smart acrylic photocatalyst coating loaded with N/C-doped $TiO_2@SiO_2$ core-shell by bio-based Tarem-rice husk waste for organic pollutant degradation. *Alexandria Engineering Journal*, *115*, 131–146. https://doi.org/https://doi.org/10.1016/j.aej.2024.12.023

Ghosh, A., Khurana, M., Chauhan, A., Takeo, M., Chakraborti, A. K., & Jain, R. K. (2010). Degradation of 4-Nitrophenol, 2-Chloro-4-nitrophenol, and 2,4-Dinitrophenol by Rhodococcus imtechensis Strain RKJ300. *Environmental Science & Technology*, *44*(3), 1069–1077. https://doi.org/10.1021/es9034123

Gurkan, Y., Kasapbasi, E., Turkten, N., & Cinar, Z. (2017). Influence of Se/N Codoping on the Structural, Optical, Electronic and Photocatalytic Properties of TiO_2. *Molecules*, *22*(3), 414.

Gurkan, Y. Y., Kasapbasi, E., & Cinar, Z. (2013). Enhanced solar photocatalytic activity of TiO_2 by selenium (IV) ion-doping: Characterization and DFT modeling of the surface. *Chemical Engineering Journal*, *214*, 34–44. https://doi.org/http://dx.doi.org/10.1016/j.cej.2012.10.025

Hui, C., Lei, Z., Xitang, W., Shujing, L., & Zhongxing, L. (2015). Preparation of Nanoporous TiO_2/SiO_2 Composite with Rice Husk as Template and Its Photocatalytic Property. *Rare Metal Materials and Engineering*, *44*(7), 1607–1611. https://doi.org/https://doi.org/10.1016/S1875-5372(15)30101-6

Kim, D. S., Han, S. J., & Kwak, S.-Y. (2007). Synthesis and photocatalytic activity of mesoporous TiO2 with the surface area, crystallite size, and pore size. *Journal of Colloid and Interface Science*, *316*(1), 85–91. https://doi.org/https://doi.org/10.1016/j.jcis.2007.07.037

Kordi, M., Farrokhi, N., Pech-Canul, M. I., & Ahmadikhah, A. (2024). Rice Husk at a Glance: From Agro-Industrial to Modern Applications. *Rice Science*, *31*(1), 14–32. https://doi.org/https://doi.org/10.1016/j.rsci.2023.08.005

Kubelka, P., & Munk, F. A. (1931). Contribution to the optics of pigments. *Zeitschrift für technische Physik*, *12*, 593–599.

Li, Z., Zheng, Z., Li, H., Xu, D., Li, X., Xiang, L., & Tu, S. (2023). Review on Rice Husk Biochar as an Adsorbent for Soil and Water Remediation. *Plants*, *12*(7), 1524.

Liou, T.-H., Liu, R.-T., Liao, Y.-C., & Ku, C.-E. (2024). Green and sustainable synthesis of mesoporous silica from agricultural biowaste and functionalized with TiO_2 nanoparticles for highly photoactive performance. *Arabian Journal of Chemistry*, *17*(6), 105764. https://doi.org/https://doi.org/10.1016/j.arabjc.2024.105764

Liou, T.-H., & Wang, S.-Y. (2025). Utilizing rice husk for sustainable production of mesoporous titania nanocomposites with highly adsorption and photocatalysis. *Biomass and Bioenergy*, *199*, 107950. https://doi.org/https://doi.org/10.1016/j.biombioe.2025.107950

Maridevaru, M. C., Sorrentino, A., Aljafari, B., & Anandan, S. (2022). Composites for Aqueous-Mediated Heterogeneously Catalyzed Degradation and Mineralization of Water Pollutants on TiO_2—A Review. *Journal of Composites Science*, *6*(11), 350.

Motamedi, M., Yerushalmi, L., Haghighat, F., & Chen, Z. (2022). Recent developments in photocatalysis of industrial effluents : A review and example of phenolic compounds degradation. *Chemosphere*, *296*, 133688. https://doi.org/https://doi.org/10.1016/j.chemosphere.2022.133688

Mujtaba, M., Fernandes Fraceto, L., Fazeli, M., Mukherjee, S., Savassa, S. M., Araujo de Medeiros, G., do Espírito Santo Pereira, A., Mancini, S. D., Lipponen, J., & Vilaplana, F. (2023). Lignocellulosic biomass from agricultural waste to the circular economy: a review with focus on biofuels, biocomposites and bioplastics. *Journal of Cleaner Production*, *402*, 136815. https://doi.org/https://doi.org/10.1016/j.jclepro.2023.136815

Nzereogu, P. U., Omah, A. D., Ezema, F. I., Iwuoha, E. I., & Nwanya, A. C. (2023). Silica extraction from rice husk: Comprehensive review and applications. *Hybrid Advances*, *4*, 100111. https://doi.org/https://doi.org/10.1016/j.hybadv.2023.100111

Okoro, H. K., Alao, S. M., Pandey, S., Jimoh, I., Basheeru, K. A., Caliphs, Z., & Ngila, J. C. (2022). Recent potential application of rice husk as an eco-friendly adsorbent for removal of heavy metals. *Applied Water Science*, *12*(12), 259. https://doi.org/10.1007/s13201-022-01778-1

Qatan, M. S., Arshad, F., Miskam, M., & Naikoo, G. A. (2024). Trends in bimetallic nanomaterials and methods for the removal of p-nitrophenol and its derivatives from wastewater. *International Journal of Environmental Science and Technology*, *21*(5), 5247–5268. https://doi.org/10.1007/s13762-023-05429-z

San, N., Hatipoğlu, A., Koçtürk, G., & Çınar, Z. (2002). Photocatalytic degradation of 4-nitrophenol in aqueous TiO_2 suspensions: Theoretical prediction of the intermediates. *Journal of Photochemistry and Photobiology A: Chemistry*, *146*(3), 189–197. https://doi.org/http://dx.doi.org/10.1016/S1010-6030(01)00620-7

Scherrer, P. (1918). Estimation of the size and internal structure of colloidal particles by means of röntgen. *Nachrichten von der Gesellschaft der Wissenschaften zu Göttingen*, *2*, 96–100.

Sing, K. S. W. (1985). Reporting physisorption data for gas/solid systems with special reference to the determination of surface area and porosity (Recommendations 1984). In *Pure and Applied Chemistry* (Vol. 57, pp. 603).

Singh Karam, D., Nagabovanalli, P., Sundara Rajoo, K., Fauziah Ishak, C., Abdu, A., Rosli, Z., Melissa Muharam, F., & Zulperi, D. (2022). An overview on the preparation of rice husk biochar, factors affecting its properties, and its agriculture application. *Journal of the Saudi Society of Agricultural Sciences*, *21*(3), 149–159. https://doi.org/https://doi.org/10.1016/j.jssas.2021.07.005

Steven, S., Restiawaty, E., & Bindar, Y. (2021). Routes for energy and bio-silica production from rice husk: A comprehensive review and emerging prospect. *Renewable and Sustainable Energy Reviews*, *149*, 111329. https://doi.org/https://doi.org/10.1016/j.rser.2021.111329

Turkten, N., Karatas, B., Karatas, Y., Cinar, Z., & Bekbolet, M. (2023). A facile synthesis of bio-inspired hierarchical microstructure TiO_2: Characterization and photocatalytic activity. *Environmental Progress & Sustainable Energy*, *42*(3), e14054. https://doi.org/https://doi.org/10.1002/ep.14054

Wang, W., Chen, H., Fang, J., & Lai, M. (2019). Large-scale preparation of rice-husk-derived mesoporous SiO_2@TiO_2 as efficient and promising photocatalysts for organic contaminants degradation. *Applied Surface Science*, *467-468*, 1187–1194. https://doi.org/https://doi.org/10.1016/j.apsusc.2018.10.275

Yalçın, Y., Kılıç, M., & Çınar, Z. (2010a). Fe^{+3}-doped TiO_2: A combined experimental and computational approach to the evaluation of visible light activity. *Applied Catalysis B: Environmental*, *99*(3-4), 469–477. https://doi.org/10.1016/j.apcatb.2010.05.013

Yalçın, Y., Kılıç, M., & Çınar, Z. (2010b). The Role of Non-Metal Doping in TiO_2 Photocatalysis. *Journal of Advanced Oxidation Technologies*, *13*(3), 281–296.

Yang, D., Du, B., Yan, Y., Li, H., Zhang, D., & Fan, T. (2014). Rice-Husk-Templated Hierarchical Porous TiO_2/SiO_2 for Enhanced Bacterial Removal. *ACS Applied Materials & Interfaces*, *6*(4), 2377–2385. https://doi.org/10.1021/am500206g

Zhang, C., Zhou, Y., Zhang, Y., Zhao, S., Fang, J., Sheng, X., Zhang, T., & Zhang, H. (2017). Double-Shelled TiO_2 Hollow Spheres Assembled with TiO_2 Nanosheets. *Chemistry – A European Journal*, *23*(18), 4336–4343. https://doi.org/https://doi.org/10.1002/chem.201602654

Zhang, H., Wang, J.-J., Fan, G., Yue, E.-L., Tang, L., Wang, X., Hou, X.-Y., & Zhang, Y. (2024). A multifunctional sensor for detecting tetracycline, 4-nitrophenol, and pesticides. *Spectrochimica Acta Part A: Molecular and Biomolecular Spectroscopy*, *322*, 124842. https://doi.org/https://doi.org/10.1016/j.saa.2024.124842

Zhang, X., Yang, Y. S., Lu, Y., Wen, Y. J., Li, P. P., & Zhang, G. (2018). Bioaugmented soil aquifer treatment for P-nitrophenol removal in wastewater unique for cold regions. *Water Research*, *144*, 616–627. https://doi.org/https://doi.org/10.1016/j.watres.2018.08.004

Zhaohui, H., Hui, C., Lei, Z., Xuan, H., Weixin, L., Wei, F., & Guanghui, W. (2018). Biogenic Hierarchical MIL-125/TiO_2@SiO_2 Derived from Rice Husk and Enhanced Photocatalytic Properties for Dye Degradation. *Photochemistry and Photobiology*, *94*(3), 512–520. https://doi.org/https://doi.org/10.1111/php.12873